ISIJ International, Vol. 48 (2008), No. 4, pp. 518–524

Structure, Mechanical Properties and Wear Resistance of High-vanadium Cast Iron

Magdalena KAWALEC and Edward FRAŚ

Chair of Cast Alloys and Composites Engineering, University of Science & Technology, Krakow, Poland.
E-mail: edfras@agh.edu.pl

(*Received on November 29, 2007; accepted on February 8, 2008*)

A series of melts with carbon content 1.38–4.16 % and that of vanadium 5.25–15.50 % was made. The X-ray diffraction of the examined alloys revealed the presence of three phases, *i.e.* ferrite, alloyed cementite, and VC_x carbide. The relationships between the content of carbon and vanadium corresponding to eutectic structure (the eutectic line) as well as the degree of eutectic saturation S_c were determined. Besides eutectics, the high-vanadium cast iron holds the following constituents in its matrix: alloyed ferrite, granular pearlite, and lamellar pearlite as well as a mixture of alloyed ferrite+granular pearlite, granular pearlite+lamellar pearlite. The results show that passing from ferritic matrix through granular pearlitic and to lamellar pearlitic matrix, hardness HB, tensile strength R_m, and yield strength $R_{0.2}$, increases while plastic properties of alloys represented by elongation A_5 decreases. The wear behaviour of alloys was tested in two different modes "specimen-abrasive paper" test (P1) and "specimen-counterspecimen" test (P2). The results obtained in test P1 are following: a) alloys with ferritic matrix and of the lowest hardness (182–189 HB) are characterised by the lowest abrasion wear resistance (s=3.14–3.93 mg/m), b) in alloys with a pearlitic matrix and hardness in the range of 387–416 HB the abrasion wear resistance is comparable to that of Hadfield cast steel (about s=2 mg/m) and c) cast iron with lamellar pearlite+granular pearlite matrix and hardness 322 to 401 HB gives the highest abrasion wear resistance of s=0.24–0.62 mg/m. In general, it can be stated that the abrasion wear in test P2 is higher than in test P1.

KEY WORDS: high-vanadium cast iron; structure; mechanical properties; wear resistance.

1. Introduction

Owing to its very good utilisation properties, cast iron remains the alloy most popular and subject to continuous development. Because of growing demand from the users of this material, the research until now has been focussed mainly on finding new grades of cast iron, always offering better mechanical and utilisation properties. The parameters that are most often changed and optimised are: physical and chemical properties in the liquid state, heat treatment of cast iron, and various alloying additives introduced to cast iron. The first trend in the research has brought a development of high-quality cast iron grades, like inoculated cast iron, cast iron with nodular graphite, and cast iron with vermicular graphite. The second trend has resulted in fabrication of cast iron with ausferritic matrix. The third trend is an attempt to solve the problem of various alloying additives that, while introduced to cast iron, can change its matrix or graphite morphology, or affect in some way the crystallisation of different carbides. The final outcome is always changing of the mechanical and utilisation properties of cast iron. One of the alloying elements that can serve this purpose is vanadium. There are only some works on the Fe–C–V systems,[1–4] nucleation of vanadium carbides[5] and structure of Fe–C–V alloys.[5,7] Until now, however, the effect of this element on the utilisation properties of cast iron has remained unclear. This fact sets the goal of the present work, which is fabrication of Fe–C–V alloys characterised by different chemical composition, analysis of their structure, and testing of their mechanical and wear resistance properties.

2. Methodology

A series of melts with carbon content changing in the range of 1.38–4.16% and that of vanadium in the range of 5.25–15.50% was made in a BALZERS (VSG 02) vacuum-type, induction furnace under argon used as a protective atmosphere. The charge for melting had the following composition: ferrovanadium with 81.7% V, Armco iron, and spectrally pure graphite. After melt overheating to a temperature of 1 700°C, foundry moulds were poured, producing rectangular test blocks (14×50×120 mm) fed from a large feeder. Moulds were made from loose, quick-setting sands with sodium silicate. From lower part of the test blocks, free from any casting defects, the test coupons were cut out to be used next in mechanical tests and metallographic examinations. The solidification temperature of the primary phases and eutectic was determined by thermal analysis on a Pt–PtRh10 thermocouple. Digital temperature recording was made on a Hewlett-Packard 34970A multichannel electronic module. From the plotted cooling curves

the values of the following parameters were recorded out: T_i - pouring temperature, T_a - austenite liquidus temperature, T_m - minimum temperature at the onset of eutectic solidification, T_b and T_e - the the beginning and the end of eutectic solidification temperature. X-ray examinations of the fabricated alloys were made using a Philips X-ray diffractometer. The measurement control and data processing were carried out by a computer system using APD program made by Philips and a JCPDS crystallographic database. The metallographic examinations were made on a LEICA MEF4M optical microscope at magnifications of 100×, 250× and 500×. The planar microstructure of eutectic alloys can be characterized by the grains count N_F (cell density), which gives the average number of eutectic grains per unit area. The N_F parameter was determined by means of the, so-called variant II of the Jeffries method, and applying the Saltykov formula as an unbiased estimator for the rectangle S of observation[8)]

$$N_F = \frac{N_i + 0.5N_s + 1}{F} \quad \text{.....(1)}$$

where: N_i is the number of eutectic grains inside S, N_s is the number of eutectic grains that intersect the sides of S but not their corners, F is the surface area, and S is measurement rectangle.

The unetched specimens were also examined under a JEOL 5500LV scanning microscope using secondary electrons (BEC). Due to this it was possible to distinguish between the vanadium carbides and other phases, the presence of which blurred to some extent the metallographic analysis. To examine in more detail the geometry of individual phases, the specimens were deep-etched with *aqua regia* and examined under a scanning microscope. The percent content of structural constituents was determined on a LEICA QWin automatic image analyser. The percent content of vanadium carbides and of the austenite dendrites transformed into ferrite was determined from photographs taken under the scanning microscope in BEC system at a large magnification. The content of the remaining structural constituents was determined from photographs taken under the optical microscope on etched specimens at a magnification of 250×. Based on the results of the metallographic examinations, a group of specimens was selected which were next subjected to static tensile test on an INSTRON type machine using an extensometer operating at a rate of 0.01 cm/min. From the plotted curves the following parameters were determined: yield strength $R_{0.2}$, tensile strength R_m and unit elongation A_5. The wear behaviour of vanadium alloys was tested in two different modes. The first "specimen-abrasive paper" test (P1) consisted in rubbing a 6×6×7 mm specimen made from the examined vanadium cast iron against a 60 corundum abrasive paper. The path of the specimen abrasive movement during one cycle was 40 m; the loading force was 10 N. Four abrasion cycles were applied to each specimen, determining each time the weight loss at an accuracy of up to 0.001 g and calculating next the mean abrasion wear coefficient, s=weight loss/path of the specimen movement. The second "specimen-counterspecimen" test (P2) used the principle of a reciprocating motion. A mandrel of 3×17 mm dimensions made from the abrasion-resistant Hadfield cast steel was moving along a path of 6 mm/cycle. For each specimen 30 000 cycles were performed, and then the weight loss was determined and the abrasion wear coefficient was calculated.

3. Results and Discussion

3.1. X-ray Diffraction

The X-ray diffraction of the examined alloys (*e.g.* **Fig. 1**) revealed the presence of three phases, *i.e.* alloyed ferrite and cementite, and VC_x carbide.

3.2. Microstructure

Table 1 gives the chemical composition of high-vanadium cast iron with structure description and content of the alloying constituents present in cast iron matrix as well as mechanical properties. Besides eutectic, depending on the C/V ratio (where C, V - content of carbon and vanadium in the cast iron, respectively, %) in high-vanadium cast iron, the presence of the following structural constituents has been detected:

1. alloyed ferrite (**Fig. 2**(a)), alloyed ferrite+granular pearlite, or granular pearlite (Figs. 2(b), 2(c)) alone, when the value of C/V is in the range of 0.1–0.2,
2. granular pearlite+lamellar pearlite, or lamellar pearlite

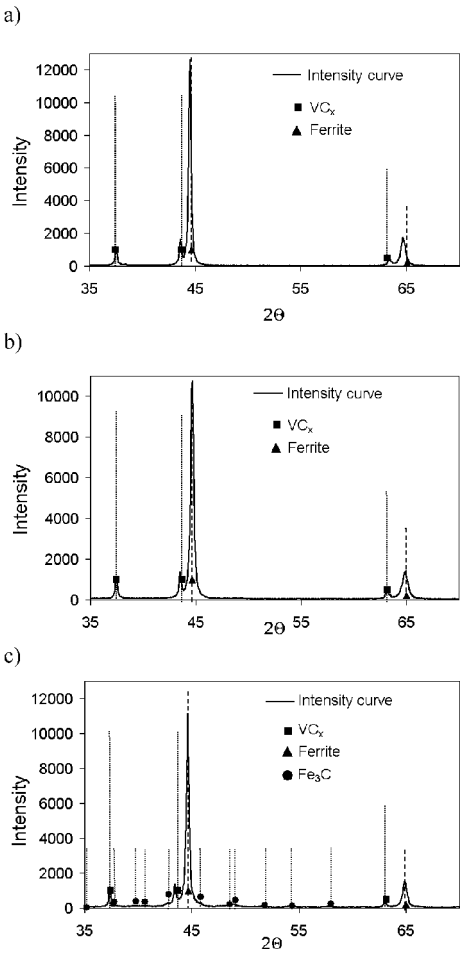

Fig. 1. Diffraction patterns of high-vanadium cast iron with matrix: a) ferritic, b) complex composed of granular and lamellar pearlite, c) complex composed of lamellar pearlite and cementite.

Table 1. Alloys chemical composition, fraction component of structure and mechanical properties.

No.	Composition		Fraction component of structure %						S_c	Properties			
	C %	V %	f_f	$f_{p,z}$	$f_{p,p}$	f_c	f_w	f_d		HB	R_m MPa	$R_{0.2}$ MPa	A_5 %
1	2.12	15.5	79.2	-	-	-	20.8	-	1.53*	175	530	259	6.0
2	1.78	15.2	81.9	-	-	-	18.1	-	1.27*	177	458	225	6.8
3	1.65	14.9	78.7	-	-	-	21.3	-	1.16*	174	550	289	5.4
4	1.53	14.7	82.1	-	-	-	17.9	-	1.07*	189	580	330	7.0
5	1.60	12.6	76.0	-	-	-	24.0	-	1.01∇	182	433	185	5.5
6	1.80	13.8	75.3	3.0	-	-	21.7	-	1.20*	-	-	-	-
7	1.87	13.3	75.1	5.0	-	-	19.9	-	1.23*	202	528	286	5.8
8	1.98	13.3	72.2	5.0	-	-	22.8	-	1.29*	180	460	212	5.3
9	1.55	10.9	76.9	5.0	-	-	18.1	23.0	0.89■	198	440	198	7.2
10	1.38	6.7	-	8.9	-	-	11.1	58.0	0.59■	283	709	556	4.2
11	1.52	8.8	-	84.4	-	-	15.6	49.0	0.76■	195	618	366	4.9
12	1.81	11.7	-	76.4	-	-	23.6	-	1.09*	-	-	-	-
13	1.73	11.6	-	82.0	-	-	18.0	-	1.04*	183	-	-	-
14	1.70	11.4	-	79.3	-	-	20.7	-	1.01∇	177	492	303	6.1
15	1.81	11.2	-	80.1	-	-	19.9	-	1.06*	194	585	306	5.1
16	1.68	11.2	-	79.6	-	-	20.4	-	0.90∇	206	-	-	-
17	2.29	11.0	-	20.1	58.3	-	21.6	-	1.33*	348	806	582	1.8
18	2.10	10.2	-	50.0	80.2	-	14.8	-	1.16*	367	-	-	-
19	2.17	9.8	-	15.0	61.9	-	23.1	-	1.17*	401	485	330	1.4
20	1.80	9.1	-	27.3	57.4	-	15.3	23.0	0.93■	322	676	535	1.1
21	2.52	9.1	-	-	78.6	-	21.4	-	1.29*	386	723	543	1.0
22	2.27	8.9	-	-	77.4	-	22.6	-	1.16*	354	768	606	1.1
23	2.03	8.5	-	-	83.7	-	16.3	-	1.00∇	382	-	-	-
24	2.58	7.8	-	-	78.2	-	21.8	-	1.20*	416	839	600	1.2
25	2.18	7.6	-	-	81.5	-	18.5	-	1.00∇	387	782	585	1.1
26	2.23	7.3	-	-	86.6	-	13.4	-	1.00∇	408	787	602	1.1
27	1.99	7.0	-	-	79.8	-	20.1	26.0	0.87■	326	718	655	0.7
28	2.73	8.8	-	-	73.0	3.0	24.0	-	1.38*	383	759	613	0.9
29	2.80	7.1	-	-	70.3	7.0	22.7	-	1.23*	430	592	-	0.5
30	2.37	6.3	-	-	78.0	5.0	17.0	20.0	0.97■	387	697	612	1.3
31	3.14	8.2	-	-	65.6	10.0	24.4	-	1.52*	413	-	-	-
32	4.16	12.5	-	-	54.9	20.0	25.1	-	2.62*	474	541	-	0.4
33	3.14	7.6	-	-	51.7	25.0	23.3	-	1.44*	437	437	-	0.2

Fractions: f_f – ferrite, f_c – cementite eutectic, f_d – austenite dendrites transformed into ferrite, $f_{p,p}$ – lamellar pearlite, $f_{p,z}$ – granular pearlite, f_w – vanadium carbides.
Structure: ■ – hypoeutectic, ∇ – eutectic, * – hypereutectic

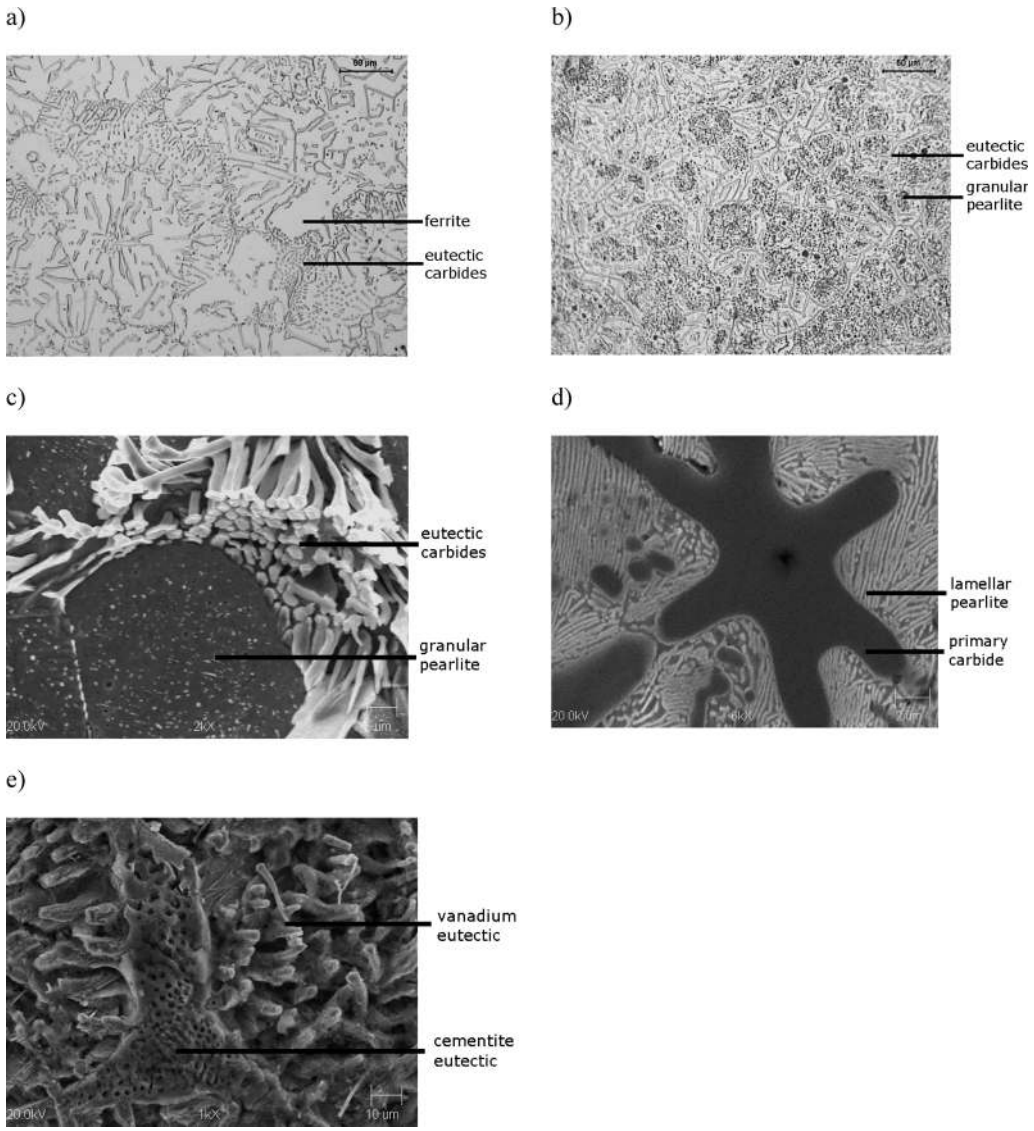

Fig. 2. The structure of high-vanadium cast iron.

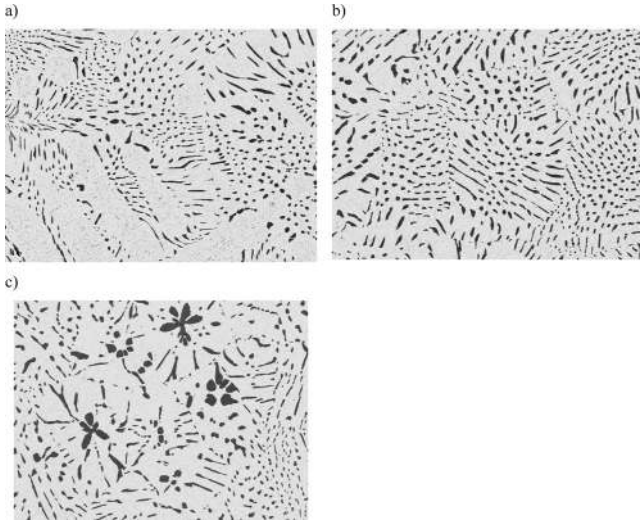

Fig. 3. The structure of high-vanadium cast iron: a) hypoeutectic, b) eutectic and c) hypereutectic.

(Fig. 2(d)) alone, when the value of C/V ratio is above 0.2,

3. alloyed cementite (Fig. 2(e)), when the value of C/V is above 0.3.

Based on the results of microscopy, the examined alloys were divided with respect to their microstructure into hyper-, hypo-, and around-eutectic. The examples of individual microstructures are shown in **Fig. 3**.

Deep etching with *aqua regia* followed by observations under the scanning microscope have proved that the the primary vanadium carbides are crystallising as non-faceted dendrites (**Figs. 4**(a), 4(b)). Eutectic grains (Figs. 4(c), 4(d)), have inside a continuous, ramified skeleton of vanadium carbides. These observations indicate, moreover, that the continuous, ramified skeleton of vanadium carbides is growing out from one common centre (**Fig. 5**) and that some fibres are, at the final stage of the grains growth, transformed into lamellar forms (Figs. 4(d) and 5(a), 5(c)). Measured grain count, N_F in test blocks ($14\times50\times120$ mm) was 55–94 mm^{-2}. In case of hypoeutectic alloys eutectic grains grow in interdendritc space (Figs. 4(e), 4(f)).

A relationship between the content of carbon and vanadium corresponding to an around-eutectic structure (the eutectic line in **Fig. 6**(a)) is described by the following equation of regression:

$$C_e = 7.91 V_e^{-0.635} \quad \text{.....(2)}$$

where C_e and V_e are carbon and vanadium content in eutectic.

The correlation coefficient of this equation is high and equals $R=0.996$.

A eutectic line obtained in our experiments is plotted in Fig. 6(b) on the phase equilibrium diagram of Fe–C–V alloys given in work.[4] The figure indicates that the points and the eutectic line obtained by experiments are shifted to the left in respect of the phase equilibrium diagram.

The degree of eutectic saturation S_c is a quotient of the carbon content in alloy C divided by the carbon content in eutectic C_e. Taking this into consideration as well as Eq. (2), the degree of eutectic saturation in high-vanadium cast iron can be determined in the following way:

$$S_c = \frac{C}{C_e} = \frac{C}{7.91 V_e^{-0.635}} \quad \text{.....(3)}$$

For $S_c<1$, $S_c=1$, $S_c>1$, we obtain hypoeutectic, eutectic and hypereutectic alloys, respectively. The values of the coefficient S_c for the obtained alloys are given in Table 1.

Figure 7 shows the effect of vanadium content on the fraction of vanadium carbides f_w in high-vanadium cast iron of around-eutectic composition and the effect of the degree of eutectic saturation S_c on the fraction f_d of the austenite

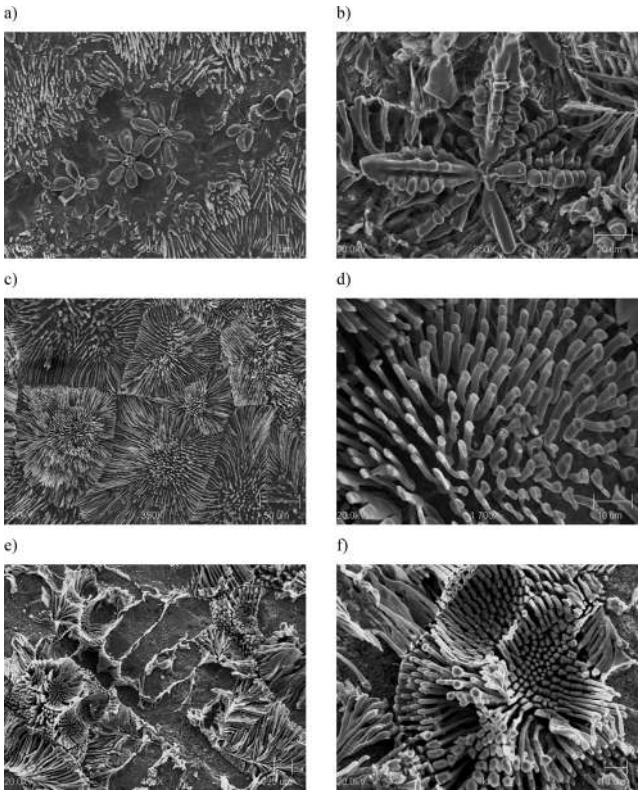

Fig. 4. The structure: (a, b) hypereutectic, (c, d) eutectic, (e, f) hypoeutectic, deep-etched with aqua regia.

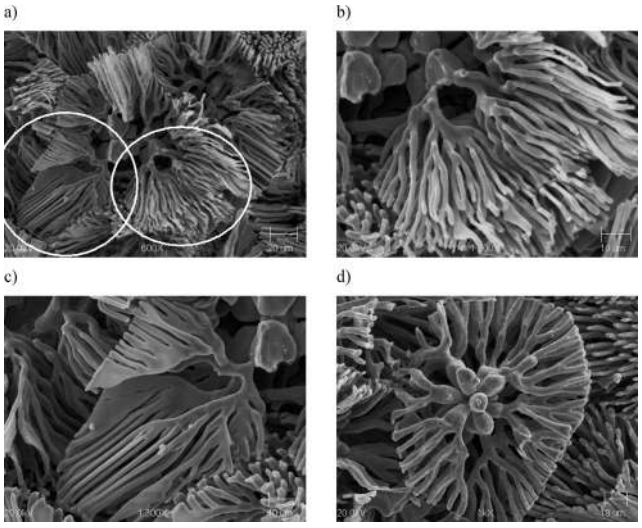

Fig. 5. The continuous, ramified skeleton of vanadium carbides growing out from one common centre, deep-etched with aqua regia.

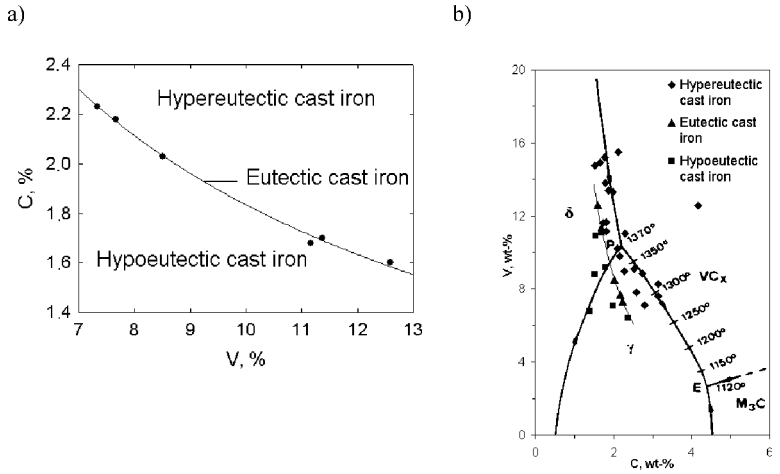

Fig. 6. The run of eutectic lines in high-vanadium cast iron (a) and projection of eutectic line against the background of Fe–C–V system (b).[4)]

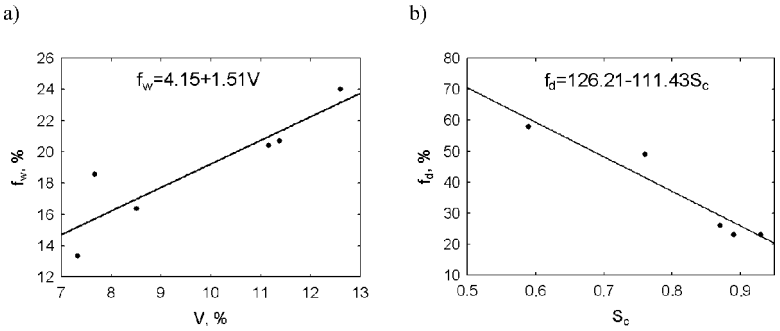

Fig. 7. The fraction of eutectic vanadium carbides in around-eutectic cast iron (a) and fraction of the austenite dendrites transformed into ferrite in hypoeutectic high-vanadium cast iron (b).

dendrites transformed into ferrite in hypoeutectic cast iron. From the figure, it follows that increasing the content of vanadium in around-eutectic cast iron makes the content of eutectic carbide VC_x increase (Fig. 7(a)), too, while increasing the degree of eutectic saturation reduces the content of the austenite dendrites transformed into ferrite (Fig. 7(b)).

3.3. Thermal Analysis

Table 2 is a compilation of the results of temperature measurements. An example of the cooling curve for high-vanadium eutectic cast iron and a differential curve are shown in **Fig. 8**(a). From Table 2 it follows that the austenite liquidus temperature, T_a, the minimum temperature, T_m at the onset of eutectic solidification, and temperature of the beginning, T_b as well as the the end, T_e of eutectic solidification, increases with increasing content of vanadium and decreasing content of carbon in Fe–C–V alloys.

3.4. Mechanical Properties

The results of the mechanical tests and mean hardness values of the fabricated alloys have been compiled in Table 1, wherefrom it follows that the matrix type exerts an important effect on the mechanical properties of cast iron. This is clearly visible in Fig. 8(b), which gives examples of the tensile curves.

According to structure type (except vanadium eutectic) as well as mechanical properties, alloys can be divided into 5 groups (**Table 3**). In general, Table 3 shows that passing from ferritic matrix through granular pearlitic and to lamellar pearlitic matrix, hardness HB, tensile strength R_m, and yield strength $R_{0.2}$, increase while plastic properties of alloys represented by elongation A_5 decrease. Moreover, presence of cementite eutectic in structure favours increase in hardness and decrease in plastic properties of alloys. It is worth mentioning that in comparison to typical white cast iron having high brittleness and which are unprocessable by typical machine tools, Fe–C–V alloys (white vanadium cast iron) are workable and show plastic properties (with ferritic matrix) which depend on vanadium carbides fraction (eutectic or primary) and type of matrix (**Fig. 9**).

Table 2. Results of temperature measurements.

No.	C %	V %	T_i °C	T_a °C	T_m °C	T_b °C	T_e °C
7	1.87	13.3	1550	1400	1363	1362	1333
13	1.73	11.6	1673	1398	1377	1377	1322
16	1.68	11.1	1628	1392	1363	1363	1335
18	2.10	10.2	1655	1396	1342	1343	1237
23	2.03	8.5	1585	1360	1331	1331	1159
25	2.18	7.6	1670	1362	1325	1325	1213
30	2.37	6.3	1512	1343	1291	1291	1159

3.5. Abrasion Wear Resistance

The results of the tests on abrasion wear resistance of high-vanadium cast iron, determined by the mean abrasion wear coefficient loss of weight, *s*, are compiled in **Table 4**. The results from test P1 were compared with the abrasion

Table 3. Effect of the matrix type on mechanical properties of Fe–C–V alloys.

No.	Structure	Properties			
		HB	R_m MPa	$R_{0.2}$ MPa	A_5 %
1-9	ferrite, ferrite + granular perlite (< 5%)	174-202	433-550	185-330	5.3-7.2
10-16	granular perlite	177-283	492-709	203-556	4.2-6.1
17-20	granular perlite + lamellar perlite	322-401	485-806	330-582	1.1-1.8
21-27	lamellar perlite	326-416	718-839	543-655	0.7-1.2
28-33	lamellar perlite + cementite eutectic	383-474	437-759	≈612	0.2-1.3

Table 4. Results of the wear resistence.

No.	Chemical composition %		Abrasion wear resistence, s mg/m	
	C	V	Test P1	Test P2
4	1.53	14.7	3.14	31.81
5	1.60	12.6	3.93	8.75
9	1.55	10.9	3.54	23.89
19	2.17	9.8	0.44	2.50
20	1.80	9.1	0.62	1.11
24	2.58	7.8	2.27	3.33
25	2.18	7.6	2.05	3.61
26	2.23	7.3	1.92	3.75
30	2.37	6.3	0.24	4.44
33	3.14	7.6	1.94	1.94
H	Hadfield cast steel		1.97	-

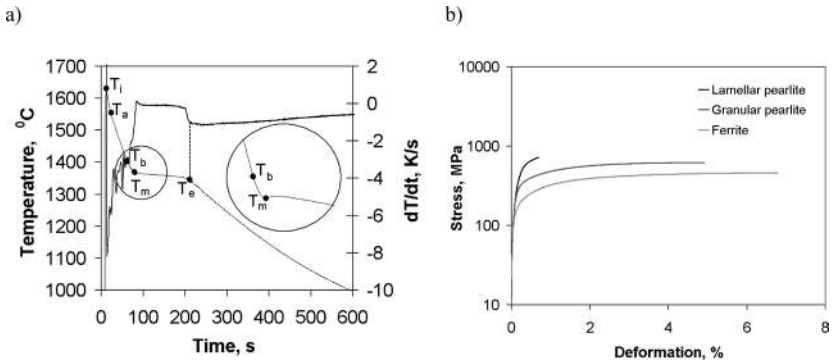

Fig. 8. Cooling curve and its derivative plotted for eutectic high-vanadium cast iron (a) and example of tensile curves plotted for high-vanadium cast iron with different types of matrix (b).

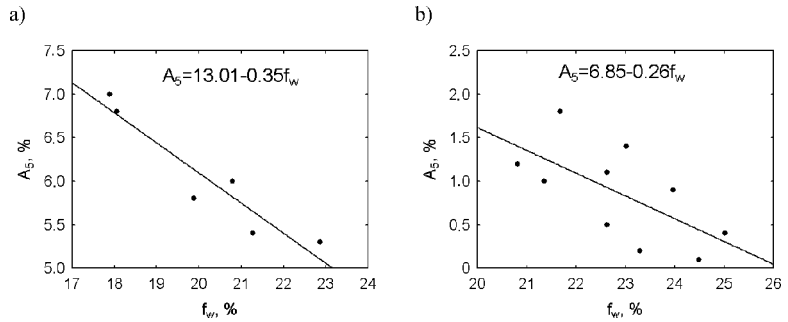

Fig. 9. Effect of vanadium carbide content (eutectic and primary) on the ductility of high-vanadium cast iron with: ferritic (a) and pearlitic (b) matrix.

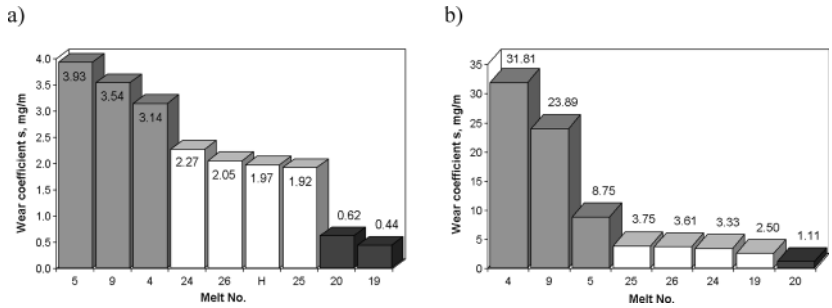

Fig. 10. Weight loss during abrasion test made for high-vanadium cast iron: specimen - abrasive paper test (P1) (a), specimen - counterspecimen test (P2) (b).

wear resistance of Hadfield cast steel; a specimen of this material was designated as H. From the conducted tests it follows that, as in the case of mechanical properties, the abrasion wear resistance of this alloy is to a great extent dependent on the type of its matrix. The results obtained in test P1 can be divided into three groups, shown on a diagram in **Fig. 10**. The first group is high-vanadium cast iron (C=1.53–1.60%, V=10.9–14.7%) from melts designated by numbers 4, 5, 9, characterised by the lowest abrasion wear resistance (s=3.14–3.54 mg/m). This group of alloys

has either a purely ferritic matrix or a ferritic matrix with small areas of granular pearlite and the lowest hardness (182–189 HB). The second group (C=2.18–2.58%, V=7.3–7.8% from melts no. 24–26) is high-vanadium cast iron of a pearlitic matrix and hardness comprised in the range of 387–416 HB; its abrasion wear resistance is comparable to that of Hadfield cast steel (about s=2 mg/m). The third group includes cast iron offering the highest abrasion wear resistance of s=0.24–0.62 mg/m (C=1.8–2.37%, V=6.3–9.8% from melts no. 19, 20); it has a lamellar pearlitic matrix and hardness comprised in the range of 322–401 HB.

Comparing the results of the abrasion wear resistance test (Table 4 and Fig. 10), a general statement can be made that the abrasion wear resistance in test P2 is higher than in test P1. This is due, first of all, to the different type of abrasion wear prevailing in each of the two tests. Like in test P1, also in test P2 the cast iron of a ferritic matrix (melts nos. 4, 5, 9) is characterised by the highest abrasion wear (s=8.75–31.81 mg/m), while the highest abrasion wear resistance (s=1.11–1.25) offer the specimens from melt no. 20. The remaining specimens were characterised by a moderate abrasion wear resistance, the difference between the moderate and poor abrasion wear resistance assuming almost tenfold values.

4. Conclusions

(1) In high-vanadium cast iron (C=1.38–4.16% and V=5.25–15.5%) the following phases have been identified: alloyed ferrite, alloyed cementite, VC_x carbides and the constituents in its matrix: alloyed ferrite, granular pearlite, and lamellar pearlite as well as a mixture of alloyed ferrite+granular pearlite, granular pearlite+lamellar pearlite.

(2) The mechanical properties of high-vanadium cast iron and its abrasion wear resistance mainly depend on the type of matrix.

(3) Dependent on the matrix, Fe–C–V alloys are characterised by a ultimate tensile strength in the range of R_m=433–839 MPa, yield strength $R_{0.2}$=185–655 MPa, hardness HB=174–474 combined with elongation A_5=0.2 do 7.2%.

(4) It is possible to obtain high-vanadium cast iron of abrasion resistance higher than that of Hadfield cast steel.

REFERENCES

1) R. Vogel and E. Martin: *Arch. Eisenhüttenwes.*, **4** (1930), 487.
2) M. J. Collins: *J. Iron Steel Inst. Lond.*, **210** (1972), 284.
3) R. Ebeling and H. Hever: *Arch. Eisenhüttenwes.*, **40**, (1969), No. 7, 551.
4) R. Kesri and M. Durand-Charre: *Mater. Sci. Technol.*, **4** (1988), 692.
5) C. R. Scerantoni and M. Boccalini: The 5th Decennial Int. Conf. on Solidification Procerssing, SP, Sheffield, (2007), 234.
6) E. Fraś and E. Guzik: *Arch. Metall.*, **25** (1980), No. 4, 757.
7) E. Fraś: Solidification of Metals, WNT, Warsaw, (2003), 233.
8) J. Ryś: Stereology of Metals, WNT, Cracow, (1995), 145.